

Investigation of antibiotic clarithromycin adsorption potential on microplastic

Zainab Ikram Sedeeq Sedeeq¹, Fatma Beduk^{1*}

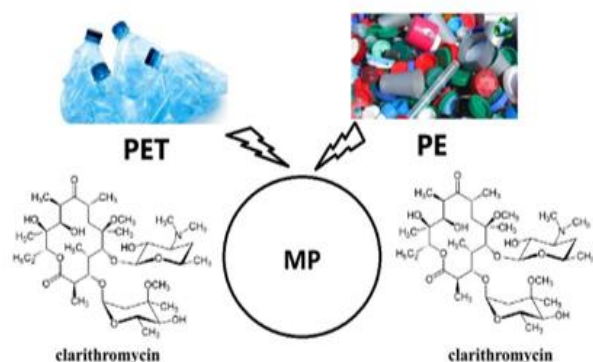
¹Necmettin Erbakan University, Engineering Faculty, Department of Environmental Engineering, Koycegiz Campus, 42060, Konya, Turkey

Received: 28/10/2024, Accepted: 18/11/2024, Available online: 19/11/2024

*to whom all correspondence should be addressed: e-mail: fabeduk@erbakan.edu.tr

<https://doi.org/10.30955/gnj.006935>

Graphical abstract



Abstract

In this study, it was aimed to investigate the potential of microplastics (MPs) to adsorb antibiotic clarithromycin (CLAR) in the water media. For this purpose, two of the most commonly used plastics; polyethylene terephthalate (PET) and polyethylene (PE) were selected. Batch adsorption experiments were performed under various conditions, i.e., pH, and ionic strength of the solution, type and dimension of MPs. Liquid chromatography equipped with mass spectrophotometry (HPLC-MS) was used for the analysis of CLAR. Fourier Transform Infrared Spectrometry (FT-IR) analysis of adsorbents was performed before and after CLAR adsorption, for chemical identification of MPs.

Results of the experimental studies showed that the adsorption reached the highest value at pH 6-7. Equilibrium adsorption time was 240 min. The adsorption occurred in accordance with pseudo-second-order kinetics. The experimental q_e values for CLAR adsorption of <2 mm PET-MPs; <5 mm PET-MPs; <2 mm PE-MPs and <5 mm PE-MPs were 0.33 mg/g, 0.26 mg/g, 2 mg/g, and 0.2 mg/g, respectively. It was determined that adsorption with <2 mm PE-MPs fits the Langmuir isotherm model ($R^2 = 0.95$), adsorption with <5 mm PE-MPs does not comply

with either Langmuir or Freundlich isotherm models, while adsorption with <2 mm PET-MPs ($R^2 = 0.74$) and <5 mm PET-MPs ($R^2 = 0.83$) fit the Freundlich isotherm model. The findings revealed that CLAR was adsorbed by all tested PET-MPs and PE-MPs, that poses an accumulation and transportation risk in the aquatic environment.

Keywords: adsorption, antibiotics, clarithromycin, isotherm, kinetic, microplastic

1. Introduction

Plastics have become one of the most important environmental pollutants due to their widespread use (Ahmad *et al.* 2020). Plastics have been widely used in industry, commerce, and construction, due to their easy molding, high mechanical and chemical resistance, and low cost. Plastics have different surface properties, various crystal degrees, and physicochemical structures depending on their polymeric properties (Fu *et al.* 2021). While only a small proportion of plastics are recycled, the remaining amount is stored in solid waste landfills, incinerated or spread out into the environment (Pacheco *et al.* 2012). Polyethylene terephthalate (PET), polyethylene (PE), polypropylene (PP), and polystyrene (PS) are the most common polymer constituents of plastics in water sources (Li *et al.* 2020). Plastics turn into microplastics (MPs) with sizes lower than 5 mm, as a result of various physicochemical and biological decomposition processes in nature (Cole *et al.* 2011).

Plastic pollution in the marine environment is one of the threats that most affects the ecosystem. Ingestion of plastics by marine fish species causes ecologically negative consequences. Young fish, mammals, sea turtles, sharks, and reptiles are often exposed to plastics in the sea, and these objects can cause their death. Seabirds are also very prone to swallow plastic objects (Lionetto and Esposito Corcione 2021). When MPs are exposed to long-term environmental weather conditions, their surface properties change (high specific surface area, porosity, amorphous structure, strong hydrophobicity, and multi-pore structure etc.) and therefore they become prone to adsorb various toxic and harmful chemicals in the

environment (Zhang *et al.* 2018). Plastics adsorb heavy metals, and various types of synthetic organic pollutants, including pharmaceuticals in aquatic environments, thus act as carriers of these pollutants (Nguyen *et al.* 2021). Plastics themselves are also sources of toxic chemicals, such as bisphenol A, phthalate, triclosan, and polybrominated diphenyl ether, that can be dissolved from their structure (Arienzo *et al.* 2021).

The use of antibiotics is increasing day by day, and their concentrations in the aquatic environment are also increasing in parallel (Aydin *et al.* 2019; Baumann *et al.* 2015). Approximately 60% of antibiotics used in human and veterinary medicine are released into the environment as parent compounds. Antibiotic residues remaining in the environment cause contamination of fresh water and food (Liu *et al.* 2022). They affect non-target organisms in the receiving environment and e.g. antibiotics develop antibiotic resistance genes (ARGs) in bacteria (Imwene *et al.* 2022).

Macrolide antibiotics are widely used in infectious diseases caused by bacterial pathogens (Zhang *et al.* 2022). It has been found that macrolide antibiotics can be poorly degraded during conventional treatment processes (Baumann *et al.* 2015). Macrolide antibiotics are used in combination with other medications to treat bacterial infections, and stomach ulcers. One of the most commonly consumed types of macrolide antibiotics is CLAR. CLAR was in the Watch List for EU, concerning water policy by Decision 2018/840. Therefore, CLAR was selected as model antibiotic in this study.

Adsorption studies of organic pollutants on different types of MPs have been carried out; Nguyen *et al.* (2021) examined the adsorption of Tetracyclines (TC), an antibiotic frequently found in aquatic environments, on high density polyethylene (HDPE) particles with an average size of 45 μm . TC adsorption on the HDPE surface was consistent with pseudo-second-order kinetics. The Langmuir adsorption isotherm described TC adsorption well ($r^2 > 0.99$). It was determined that chemical adsorption and hydrogen bond formation were responsible for the interaction between TC and HDPE surface. Maximum TC adsorption occurred at pH 7.0. It was evaluated that the overall adsorption energy was 1.0 kJ-mol, which means that TC adsorption on the PE surface occurred thermodynamically. The presence of foreign ions increased TC adsorption due to compression of the electrical double layer and complex formation (such as Mg^{2+} and Ca^{2+}). The presence of dissolved organic matter also affected the TC adsorption to increase by a small amount.

Chen *et al.* (2021) determined TC adsorption potential of PE particles by using laboratory experiments and molecular dynamics simulation. As a result of the analysis of adsorption kinetics and adsorption thermodynamics investigated by FT-IR and X-ray photoelectron spectroscopy (XPS), it was stated that the adsorption behavior of TC occurred only on PE surface and the adsorption process could be explained mainly by the intermolecular van der Waals force and the filling mechanism of micropores.

Atugoda *et al.* (2020) conducted a research study about adsorption of ciprofloxacin (CIPRO) on PE-MPs. In the study, the effects of pH, ionic strength and natural organic matter on adsorption efficiency were evaluated. The maximum adsorption of CIPRO onto PE-MPs was observed around pH 6.5-7.5. As a result of experiments investigating the effect of ionic strength, it was determined that 0.1 M NaNO_3 caused a 17% reduction in CIPRO adsorption. Addition of humic acid (HA) to the medium reduced the adsorption potential by 89%. This was explained by CIPRO's higher affinity for complexation with HA. It was determined that CIPRO has a physical sorption on PE-MPs. In this case, it was evaluated that small environmental changes could cause desorption of CIPRO from MPs.

Li *et al.* (2018) determined the adsorption potential of 5 antibiotics [sulfadiazine (SDZ), Amoxicillin (AMX), TC, CIPRO and Trimethoprim (TMP)] on 5 types of MPs [PE, PS, PP, polyamide (PA), polyvinyl chloride (PVC)] in freshwater and seawater systems. SEM and X-ray diffractometer (XRD) analysis were used for the characterization of MPs. As a result of the study, it was determined that PA had the strongest adsorption capacity for antibiotics. Adsorption showed a positive correlation with the porous structure of the adsorbent, hydrogen bonds and octanol-water partition coefficients (Log Kow). Compared with the freshwater system, the adsorption capacity in seawater was significantly reduced. The results showed that PA particles, commonly observed in waters, could serve as antibiotic carriers in the aquatic environment.

The presence of MPs in aquatic environment, their contribution to the transport of pollutants and their effects on aquatic organisms have been studied in recent years. However, a very limited number of studies have been conducted on the adsorption of antibiotics on different types of MPs. In this study, it was aimed to investigate the antibiotic CLAR adsorption potential of the most common type of MPs; PET and PE in the water media.

2. Materials and methods

2.1. Materials and chemicals

Certified reference materials of antibiotic (PHR1038) was provided from Merck. Methanol CH_3OH (Merck, Germany) was used to dissolve the antibiotic. 5 mM ammonium formate NH_4HCO_2 ($\geq 99.0\%$ for HPLC) and 0.1% formic acid were used as mobile phase for HPLC. 0.1 M sodium hydroxide (NaOH) and 0.1 M hydrochloric acid (HCl) were used to adjust pH (Merck, Germany). Sodium chloride (NaCl) (Merck, Germany) was used to determine the effect of ionic strength.

PET used as adsorbent was obtained from 500 mL water bottles commercially available in the market. PET was washed with pure water and dried before use. PET was grinded in a grinder and those that passed through a 5 mm sieve were used as <5 mm PET-MPs (named as 5 mm PET-MPs), and those that passed through a 2 mm sieve were used as <2 mm PET-MPs (named as 2 mm PET-MPs).

PE used as adsorbent was obtained from a recycling facility. PE pellets were first washed with pure water and dried. Those that passed through a 5 mm sieve were used in their current pellet form (named as 5 mm PE-MPs), and those that passed through a 2 mm sieve were used as <2 mm PE-MPs (named as 2 mm PE-MPs).

2.2. Characterization of MPs

Surface chemical characterizations of PET-MPs and PE-MPs before and after CLAR adsorption were determined by FT-IR spectroscopy. Measurements were made in the range of 400–4000 cm^{-1} , with 16 repeated scans and a resolution of 4 cm^{-1} . FT-IR spectroscopy is basically based on the absorption of infrared light by the substance being examined.

Surface physical characterizations of PET-MPs and PE-MPs were determined by SEM. The surface morphology of the samples were imaged at different magnifications at 20 kV., Hitachi-SU 1510. Since the PET-MPs and PE-MPs used in this study were not conductive, they were coated with a very thin (approximately 3 Å/second) conductive material under 20 kV vacuum, so as to be examined.

Surface area and porosity of the MPs were measured using the Brunauer, Emmett and Teller (BET) method in a liquid nitrogen environment at 77 K, based on nitrogen (N_2) gas adsorption technique. Thanks to adsorption and desorption capacities, BET surface area and pore size distribution could be determined. BET analysis of PET-MPs and PE-MPs used in this study were carried out at 30 °C for 24 hours.

2.2.1. Adsorption experiments

3 g/L suspensions were prepared by adding 2 mm and 5 mm PET-MPs, and 2 mm and 5 mm PE-MPs to 50 mL distilled water in 100 mL glass vials. After spiking the initial concentration of 6 mg/L CLAR to the solution, pH at which optimum CLAR adsorption occurs was found, by adjusting the pH of the solution to a range of 4-8, using 0.1 M HCl or NaOH. Batch adsorption experiments were carried out in a controlled environment at 25 °C with a shaking speed of 220 rpm with a horizontal shaker (Shin Saeng, Korea), for 4 h. Withdrawn samples were filtered through PTFE membrane syringe filters, with pore size of 0.45 μ (Sartorius, SRP25), to remove MPs. Filtrate samples were analyzed for CLAR, by the HPLC-MS (Agilent Technologies). The adsorption kinetics were determined with an initial CLAR concentration of 6 mg/L, and MPs dosage of 3 g/L, at the optimum pH6-7, determined in the previous experimental step. Samples were withdrawn at the time intervals of 15, 30, 45, 60, 90, 180, 240, etc. min., filtered through 0.45 μ PTFE filters, and subjected to CLAR analysis. The adsorption isotherms were determined with CLAR concentration ranging between 2-30 mg/L. MPs dosage was kept as 3 g/L and the pH was adjusted to 6-7. Vials were kept on horizontal shaker for 240 min., which was equilibrium time, determined by the kinetics experiments. To determine the effect of environmental conditions on adsorption, the effects of ionic strength (0.01; 0.1; 1 M NaCl) were examined under optimum experimental conditions. All experiments were conducted

in duplicate and results were given as mean. Adsorbed amount of antibiotics and percentage of the removal were calculated by using Eq (1) and Eq (2), respectively.

$$q_e = \frac{C_o - C_e}{m} \times V \quad (1)$$

$$\% \text{ Removal} = \frac{C_o - C_e}{C_o} \times 100 \quad (2)$$

Where; q_e is the adsorbed amount of antibiotic at equilibrium (mg/g), C_o is the initial concentration of antibiotic (mg/L), C_e is the equilibrium concentration of antibiotic (mg/L), m is the amount of adsorbent (g), V is the solution volume (L).

2.3. Sorption Models

Adsorption kinetic models have been used to investigate the adsorption mechanisms of pollutants on adsorbents (Fu *et al.* 2021). The analysis of adsorption kinetics helps to estimate the equilibrium time and determine the adsorption rate of a solute by an adsorbent (Zhang *et al.* 2020). Adsorption rate is an important parameter for the evaluation of the adsorption efficiency. The most commonly used adsorption kinetic models are pseudo-first-order kinetic model and pseudo-second-order kinetic model (Fu *et al.* 2021). The formulas of pseudo-first-order and pseudo-second-order kinetic models are given in Eq (3) and Eq (4), respectively (Ho and McKay 1999).

$$\ln = (q_e - q_t) = \ln q_e - k_1 t \quad (3)$$

$$q = \frac{k_2 q_e^2 t}{1 + k_2 q_e t} \quad (4)$$

Here:

q_e : The amount of compound adsorbed at equilibrium (mg/g)

q_t : The amount of compound adsorbed at time t (mg/g)

k_1 : Pseudo-first-order rate constant (1/min)

k_2 : Pseudo-second-order rate constant (1/min)

t : Contact time (min)

Adsorption isotherms are generally used to estimate the amount of adsorbate that can be adsorbed on a solid surface and to determine whether the adsorption mechanism is linear single-layer or multilayer adsorption (Fu *et al.* 2021). Langmuir and Freundlich adsorption isotherm models have been widely used to determine the adsorption isotherms of antibiotics (Li *et al.* 2018). The Langmuir isotherm was primarily used to describe the adsorption between gases and solid surfaces and to determine the adsorption capacity of the adsorbent. This isotherm assumes that adsorption occurs in monolayer homogeneous regions on the adsorbent. According to this model, adsorption and desorption occur in equilibrium (Langmuir 1918). The Freundlich isotherm assumes that adsorption occurs in multilayer heterogeneous regions on the adsorbent. According to this model, the heat of

adsorption and affinity are not distributed uniformly on the heterogeneous surface and the adsorption is reversible (Freundlich 1906).

The linear form of the Langmuir and Freundlich adsorption isotherm models are given in Eq. (5), and Eq. (6), respectively.

Langmuir isotherm model:

$$\frac{C_e}{q_e} = \frac{1}{(q_e k_L)} + \frac{C_e}{q_e} \quad (5)$$

$$\ln q_e = \ln k_f + \frac{1}{n \ln C_e} \quad (6)$$

Here:

C_e : Compound concentration at equilibrium (mg/L)

q_e : Adsorbed amount of compound at equilibrium (mg/g)

k_L : Langmuir adsorption constant (L/mg)

k_f : Freundlich partition ratio (mg/g)

n : Freundlich adsorption constant; surface heterogeneity factor

2.4. Analytical method

Liquid chromatography equipped with a mass spectrophotometer was used for quantitative analysis of target compounds (HPLC-MS, Agilent Technologies). The optimum column temperature program and carrier liquid of the system were determined by using CLAR standard solution at a concentration of 10 mg/L. Chromatographic separation was performed with an Agilent Poroshell 120 EC-C18 (100 mm x 3 mm, particle size 2.7 μ m) column. The calibration curve was prepared using seven standard solutions in the linear range. It was aimed to obtain linear results in the concentration range studied. Each sample was analyzed in duplicate.

Antibiotics were studied in positive mode and the most suitable carrier phase A was water containing 0.1% formic acid and 5 mM ammonium formate, and carrier phase B was methanol. The most suitable carrier phase flow rate was determined to be 0.6 mL/min. The initial carrier phase ratio was 90% (A): 10% (B) and was kept at this ratio for 1 min. Then, carrier phase B was increased linearly to 30% in 3 minutes, to 70% in 8 min., to 95% in 2 min. and kept at this rate for 2 min. The initial carrier phase conditions were returned and the study was carried out under these conditions for 4 min. before the next injection. The column temperature was 35 °C and the injection volume was 2 μ L. The protonated product ion [M+H]⁺ was detected by injecting each compound prepared at a concentration of 10 ng/ μ L into the standard HPLC-MS system in scan mode.

Table 1 shows the retention times (RT) and mass to charge ratio (m/z) values for antibiotic under optimum HPLC-MS conditions. **Figure 1** shows the standard chromatogram of antibiotic CLAR under optimum HPLC-MS conditions. Limit of detection (LOD) and limit of quantification (LOQ) values for the CLAR were determined

to be 3.8×10^{-6} ng/L, and 1.27×10^{-5} ng/L. It was seen that R² values varied between 0.9928-0.9998. Relative standard deviation (RSD) of repeatability values ranged between 1.52% and 9.12% (n=6).

Table 1. Retention time and m/z values for antibiotic CLAR under optimum HPLC-MS conditions

Antibiotic	m/z	RT (min)
CLAR	748, 590 [M+H] ⁺	14.288



Figure 1. Standard chromatogram for antibiotic CLAR under optimum HPLC-MS conditions (10 ng/ μ L)

3. Results and discussion

3.1. Characterization of PET-MPs and PE-MPs

3.1.1. Morphology and surface area of PET-MPs and PE-MPs

Surface morphology images of 2 mm and 5 mm PET-MPs and 2 mm and 5 mm PE-MPs samples with SEM at 20 kV at different magnifications are given in **Figure 2** and **Figure 3**, respectively. Multiple irregular folds on particle surfaces create more voids and pore spaces, therefore exhibit higher numbers of adsorption sites. PET-MPs and PE-MPs samples showed low crystallinity. This allows antibiotic molecules to be adsorbed into the loosely arranged polymer structure by Van der Waals forces (Nguyen *et al.* 2021; Atugoda *et al.* 2020; Fu *et al.* 2021). As a result of multi-point BET analysis, the surface area of 2 mm PET-MPs was 0.002 m²/g, while it was 0.235 m²/g for 2 mm PE-MPs. The surface area of 5 mm PET or PE-MPs could not be determined by multi-point BET analysis method. As a result of the analysis performed with the density function theory (DFT method), the surface areas of 5 mm PET-MPs and 5 mm PE-MPs were determined as 0.145 m²/g and 0.126 m²/g, respectively.

3.1.2. FT-IR analysis of PET-MPs and PE-MPs

FT-IR spectra of PET-MPs and PE-MPs before and after CLAR adsorption are given in **Figure 4**. The most frequently detected peaks were in the range of 700-3800 cm⁻¹. The region between 400-1500 (fingerprint region) represents specific compounds and the region between 1500-4000 (functional group region) represents the existing chemical bond types (Dovbeshko *et al.* 2000; Movasaghi *et al.* 2008). Significant FT-IR peaks and the identified functional groups of PET-MPs and PE-MPs before and after CLAR adsorption are given in **Table 2**. The point with the highest vibration in the FT-IR spectra and the highest peak was defined as the adsorption frequency.

CLAR adsorption of 2 mm PET-MPs; 5 mm PET-MPs, 2 mm PE-MPs, and 5 mm PE-MPs occurred at 1725 cm^{-1} , 1000 cm^{-1} , 2900 cm^{-1} , and 2900 cm^{-1} frequencies, respectively. Carboxyl and vinyl ether compounds were identified in PET samples, and alkane compounds were identified in PE samples. C=O and C-H stretching and C-O ribose bond

were detected. FT-IR analysis of MPs revealed that the spectra of the analyzed particles matched the corresponding spectra for PET and PE in the instrument database. Therefore, MP samples were characterized to confirm the specifications provided by the manufacturer.

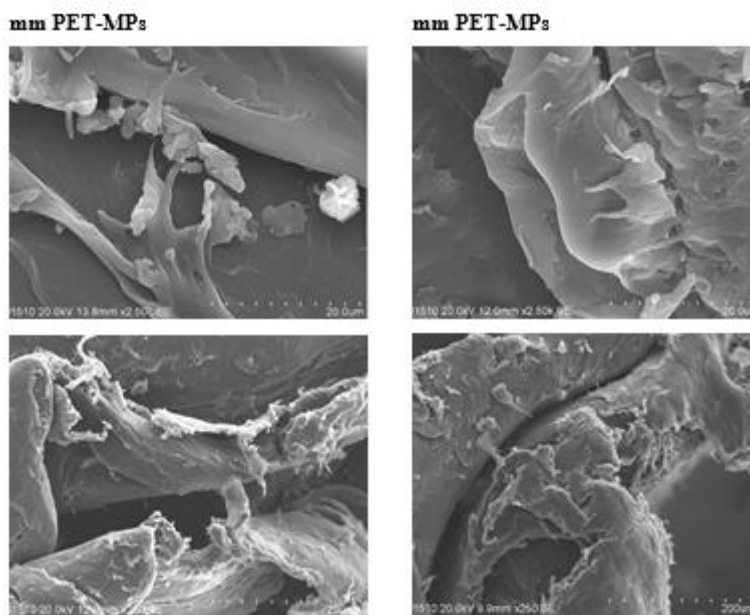


Figure 2. SEM images of 2 mm PET-MPs and 5 mm PET-MPs

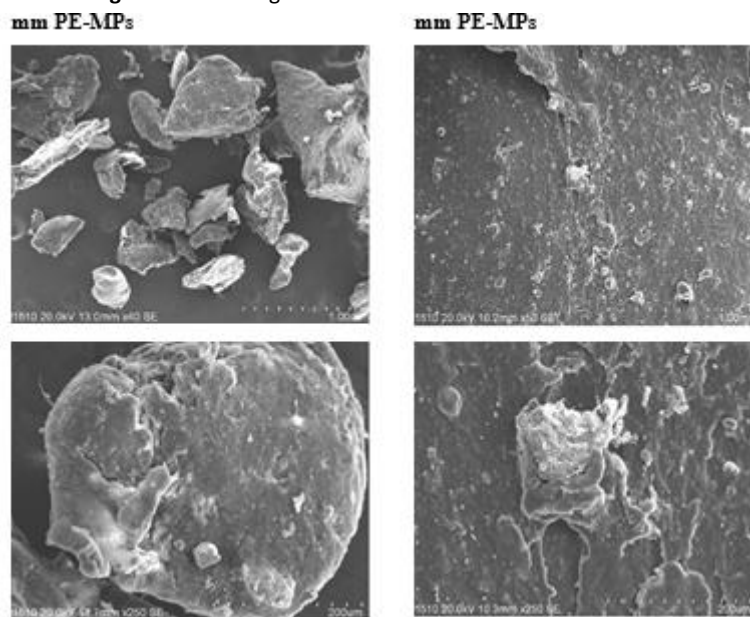


Figure 3. SEM images of 2 mm PE-MPs and 5 mm PE-MPs

Table 2. Significant FT-IR peaks and identified functional groups of PET-MPs and PE-MPs before and after CLAR adsorption

MPs	Before Adsorption (cm^{-1})	After Adsorption (cm^{-1})	CLAR (cm^{-1})	Adsorption Frequency (cm^{-1})	Functional group	Compounds
2 mm PET	1718.85	1712.91	1732.67	1725	(C=O stretching)	Carboxyl
5 mm PET	1015.91	1011.82	1010.63	1000	(C-O Ribose bond)	Vinyl Ether
2 mm PE	2915.56	2915.87	2916.98	2900	(C-H stretching)	Alkane
5 mm PE	2916.12	2918.18	2916.98	2900	(C-H stretching)	Alkane

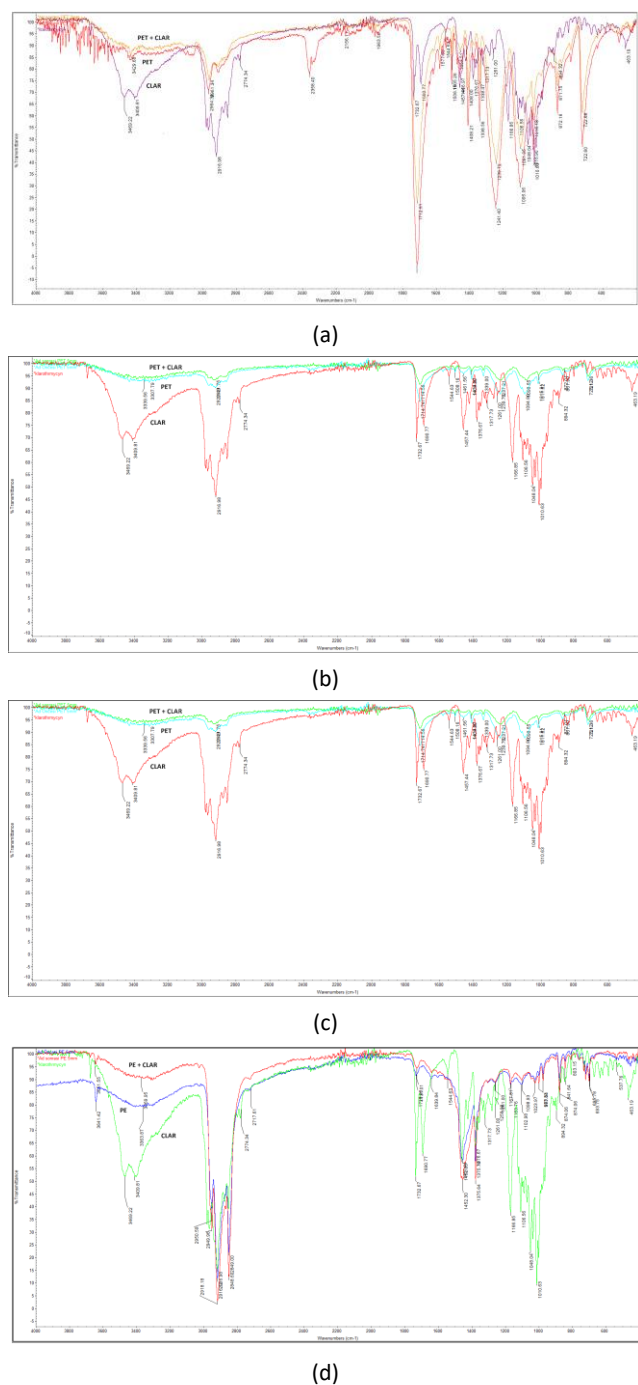


Figure 4. FT-IR spectra of PET-MPs and PE-MPs before and after CLAR adsorption (a: 2 mm PET-MP + CLAR; b: 5 mm PET-MP + CLAR; c: 2 mm PE-MP + CLAR; d: 5 mm PE-MP + CLAR)

3.2. Effect of pH on CLAR Adsorption

Antibiotics are ionizable compounds. The ionization constant (pKa) of various antibiotics often varies significantly due to their specific functional groups. Antibiotics can exist as cations, zwitter ions, or anions depending on solution pH. Therefore, under a certain pH condition, the speciation of ionic chemicals can affect their sorption degree on MPs, since electrostatic interaction occurs at a certain pH (Li *et al.* 2018; Fu *et al.* 2021; Atugoda *et al.* 2020). The CLAR adsorption capacity of PET-MPs and PE-MPs was tested in the solution pH range of 2-11. It was determined that the CLAR was decomposed at pH 2 and pH 11. Therefore, the results obtained in the pH4-9 range were evaluated (**Figure 5**). In

this pH range, cationic form of CLAR (pKa = 8,99 at 25 °C) lead to electrostatic interaction between CLAR and plastics. The surfaces of MPs are negatively charged. Therefore, ions in the medium can electrostatically bind to the binding sites and disrupt the charge balance of the surface (Moura *et al.* 2022). Adsorption capacity was increased under acid-normal conditions and maximum adsorption was achieved between pH6-7 similar to reported by Chen *et al.* (2021) for adsorption of tetracyclins (TC) on PE-MPs. When pH exceeded 7 and decreased below 6, the adsorption capacity of MPs decreased. The removal rates were determined as 7% for 2 mm PET-MPs, and 85% for 2 mm PE-MPs at pH6-7. If the pH of the adsorption medium exceeds the zero charge point (pHpzc) of MPs, their surfaces will be negatively charged and electrostatically attract positively charged organic pollutants. However, when the pH of the adsorption medium exceeds the acid dissociation constant (pKa) of organic pollutants, the pollutants will be deprotonated and enter an anionic form, which will cause electrostatic repulsion and prevent their adsorption by MPs. Therefore, electrostatic interaction is closely related to the electrification of MPs, the shape of organic pollutants, and the amount of charge involved (Fu *et al.* 2021). In the study conducted by Nguyen *et al.* (2021), the effect of pH on TC adsorption of PE particles was investigated. It was noted that the surface of PE particles was negatively charged at pH > pH_{ZPC} (~1.8) and as a result, the TC adsorption capacity was found to increase with pH, reaching a maximum value of 6.4 mg/g at pH 7.0, then decreasing with further increase in pH. The results show that TC was predominantly positively and neutrally charged at pH < 3.3 and 3.3 < pH < 8, respectively.

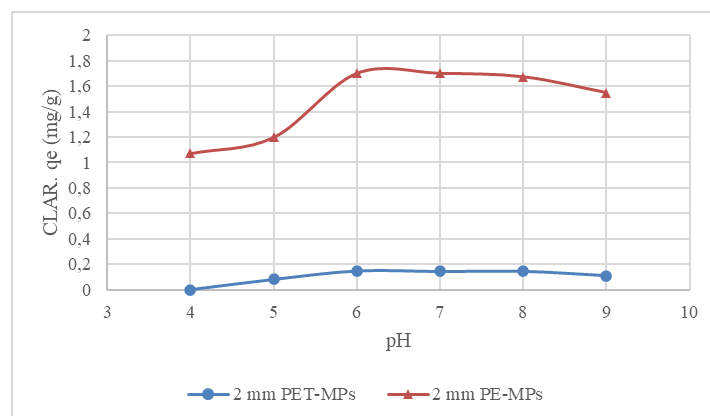


Figure 5. Effect of pH on the adsorption of CLAR on PET-MPs and PE-MPs (Experimental conditions; adsorbent: 3 g/L, adsorption time: 4 hours, C₀: 6 mg/L CLAR, sample volume: 50 mL, pH adjustment with 0.1 M HCl, 0.1 M NaOH, stirring speed: 220 rpm, temperature: 25 °C, n=2)

3.3. Adsorption Kinetics

Findings of kinetic studies allowed to obtain information about adsorption rate of CLAR on MPs. **Figure 6** indicates the sorption percent of CLAR as a function of contact time. Results show that equilibrium time was achieved in 240 min. When 65% adsorption rate was observed in just 15 min with 2 mm PE-MPs, adsorption rate went up to nearly 90% in 240 min. Lower adsorption rates were

observed for both 2 mm PET-MPs and 5 mm PET-MPs, which were nearly 17% and 13%, respectively. q_e values determined at equilibrium time for PET-MPs-2 mm, PET-MPs-5 mm, PE-MPs-2 mm, and PE-MPs-5 mm were 0.33 mg/g, 0.26 mg/g, 2 mg/g, and 0.2 mg/g, respectively. Lower adsorption value observed for PE-MPs-5 mm was attributed to smoother surface morphology observed by SEM images (Figure 3). Adsorption of CLAR on PE-MPs was also examined by Atugoda *et al.* (2020). 3 mg/g CLAR adsorption on PE-MPs in zero ionic strength and pH 7 was reported.

When the compatibility of the adsorption temporal change data with the pseudo-first-order order and pseudo-second-order kinetic models was evaluated, it was found that the adsorption was compatible with the

pseudo-second-order kinetic model for all tested MPs (Figure 7). In the graphs drawn using t against t/q_t data, r^2 values varied between 0.98-0.99. The rate constants (k_1 and k_2) and theoretical equilibrium sorption capacities for CLAR ($q_{e_{calculated}}$) were calculated by use of the slopes and intercepts of the linear plots of the pseudo first-order and pseudo-second-order kinetic models. It was found that the experimentally determined q_e values ($q_{e_{experimental}}$) were significantly overlapping with the q_e values calculated with the pseudo-second-order kinetic model (Table 3). However, the calculated q_e and the experimental q_e did not match in the results obtained with PE-MPs-5 mm, which could be explained by the very low levels of adsorption.

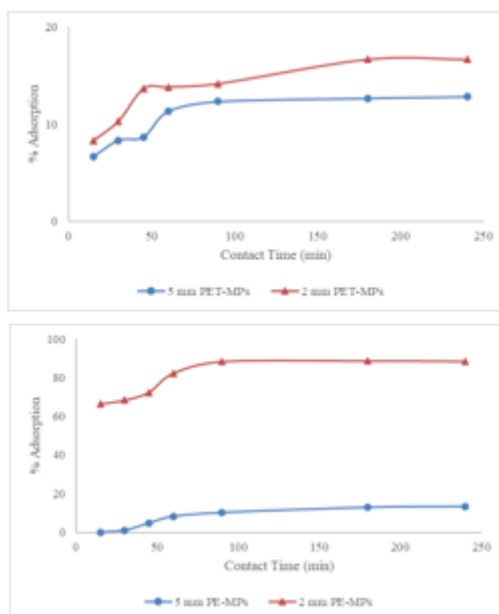


Figure 6. Effect of contact time on adsorption of CLAR by PET-MPs and PE-MPs (Experimental conditions; adsorbent: 3 g/L, adsorption time: 15, 30, 45, 60, 90, 180, 240 min, C_0 : 6 mg/L CLAR, sample volume: 50 mL, pH 6.0-7.0, stirring speed: 220 rpm, temperature: 25 °C, n=2)

Table 3. Sorption rate constants and equilibrium sorption capacities for pseudo-first-order and pseudo-second-order kinetic models

	2 mm PET-MPs	5 mm PET-MPs	2 mm PE-MPs	5 mm PE-MPs
$q_{e_{experimental}}$ (mg/g)	0.33	0.26	2.0	0.2
<i>Pseudo-first-order kinetic constants</i>				
k_1 (1/min)	0.0072	0.01	0.0031	0.02
$q_{e_{calculated}}$ (mg/g)	5.5	6.3	1.5	2.0
R^2	0.79	0.92	0.74	0.20
<i>Pseudo-second-order kinetic constants</i>				
k_2 (g/mg.min)	0.002	0.001	0.59	1.97×10^{-8}
$q_{e_{calculated}}$ (mg/g)	0.36	0.27	2.11	0.0004
R^2	0.99	0.99	0.99	0.98

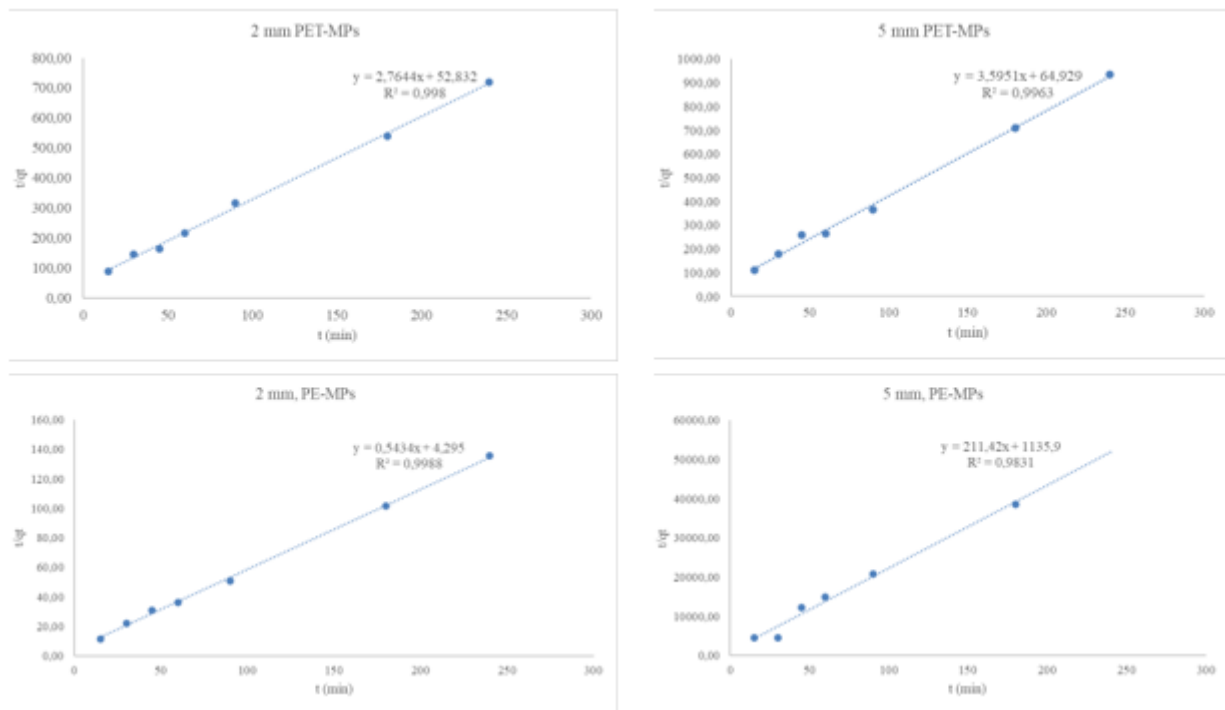


Figure 7. Pseudo-second-order kinetic model of CLAR adsorption by PET-MPs and PE-MPs (Experimental conditions; adsorbent: 3 g/L, adsorption time: 15, 30, 45, 60, 90, 180, 240 min, C_0 : 6 mg/L CLAR, sample volume: 50 mL, pH 6.0-7.0, stirring speed: 220 rpm, temperature: 25 °C, $n=2$)

3.4. Adsorption isotherms

The experimental results were analyzed by using Langmuir and Freundlich isotherm models, so as to evaluate the event that governs the adsorption between the adsorbent and adsorbate in the solution. For this purpose, the adsorption capacities of PET-MPs and PE-MPs in the solution with a C_0 concentration of 2-20 mg/L CLAR were determined at equilibrium time. Langmuir and Freundlich isotherm parameters are given in **Table 4**. It was determined that 2 mm PE-MPs complies with the Langmuir isotherm model ($r^2=0.94$), while 2 mm PET-MPs ($r^2=0.73$) and 5 mm PET-MPs ($r^2=0.83$) comply with the Freundlich isotherm model. 5 mm PE-MPs does not comply with either Langmuir, or Freundlich isotherm models. Linear regression graphs of PET-MPs and PE-MPs for the Langmuir and Freundlich isotherm models are given in **Figure 8** and **Figure 9**, respectively. CLAR adsorption with 2 mm PE-MPs comply with the Langmuir isotherm model assumes that adsorption occurs in

monolayer homogeneous regions on the adsorbent. According to this model, adsorption and desorption occur in equilibrium. The conformity of CLAR adsorption with 2 mm PET-MPs and 5 mm PET-MPs to the Freundlich isotherm model reveals that the adsorption occurs in multilayer heterogeneous regions on the adsorbent. According to this model, the adsorption heat and affinity are not uniformly distributed on the heterogeneous surface and the adsorption is reversible.

When the studies in the literature are examined, it is generally determined that the adsorption of pharmaceuticals on plastics obeys the Langmuir and Freundlich isotherms. The adsorption of TC antibiotic on HDPE with a size of 45 μm was investigated by Nguyen *et al.* (2021). The conformity of the adsorption to the linear, Langmuir and Freundlich isotherms was evaluated. The obtained results showed that the adsorption was more suitable for the Langmuir isotherm model ($r^2=0.99$).

Table 4. Langmuir and Freundlich isotherm parameters

	2 mm PET-MPs	5 mm PET-MPs	2 mm PE-MPs	5 mm PE-MPs
Langmuir Isotherm Model				
q_{max} (mg/g)	0.049	0.383	2.299	0.004
k_L	4316	33.582	30.618	790403
R^2	0.13	0.44	0.94	0.04
Freundlich Isotherm Model				
k_F (mg/g)	35.53	22.95	1.78	2598.4
n	0.76	1.00	6.14	0.58
R^2	0.73	0.83	0.25	0.49

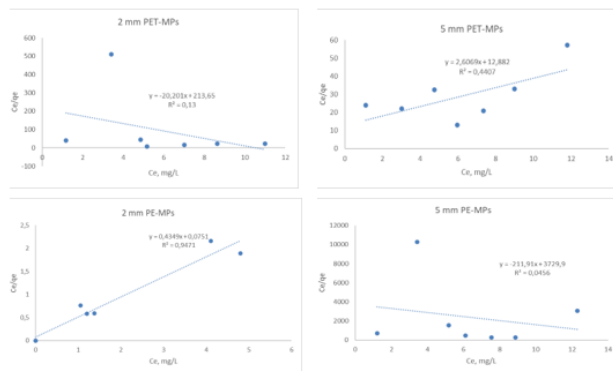


Figure 8. Langmuir isotherm graphs of CLAR adsorption with PET-MPs and PE-MPs (Experimental conditions; adsorbent: 3 g/L, adsorption time: 240 min, C₀: 2-20 mg/L CLAR, sample volume: 50 mL, pH 6.0-7.0, stirring speed: 220 rpm, temperature: 25 °C, n=2)

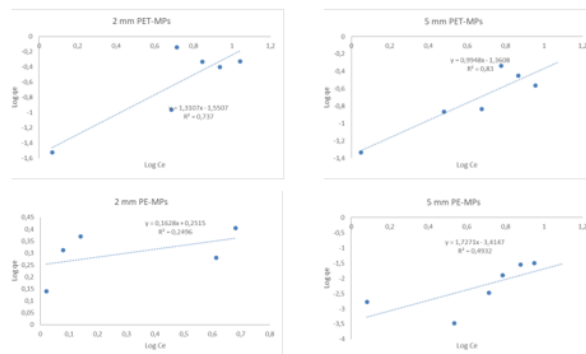


Figure 9. Freundlich isotherm graphs of CLAR adsorption with PET-MPs and PE-MPs (Experimental conditions; adsorbent: 3 g/L, adsorption time: 240 min, C₀: 2-20 mg/L CLAR, sample volume: 50 mL, pH 6.0-7.0, stirring speed: 220 rpm, temperature: 25 °C, n=2)

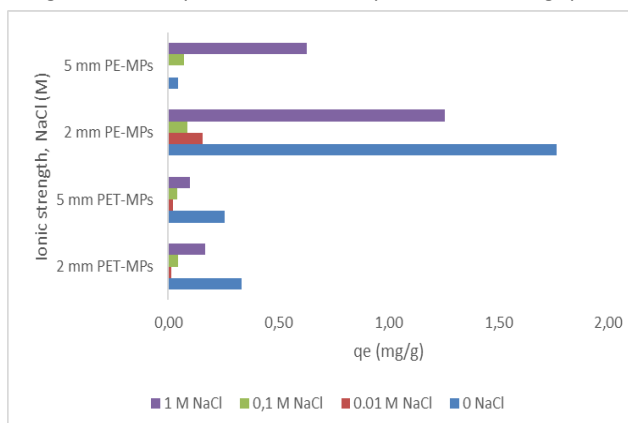


Figure 10. Effect of ionic strength on CLAR adsorption (Experimental conditions; adsorbent: 3 g/L PE-MPs and PET-MPs, pH6.0-7.0, adsorption time: 4 hours, C₀: 10 mg/L CLAR, sample volume: 50 mL, ionic strength: 0.01 M NaCl, 0.1 M NaCl, 1 M NaCl, stirring speed: 220 rpm, temperature: 25 °C, n = 2)

3.5. Effect of Ionic Strength on CLAR Adsorption

In general, the ionic strength of the solution is quite low in adsorption experiments of pharmaceuticals, carried out with distilled water. However, salinity and hence ionic strength vary greatly in natural waters. Freshwater sources have significantly less dissolved salt than sea or ocean waters. Therefore, the pharmaceuticals adsorption capacity of MPs may differ significantly depending on their entry point into the environment. MPs have different entry points into the natural environment; usually discharged into the rivers or lakes via wastewater treatment plants and in some cases, directly into the seas and oceans (Klavins *et al.* 2022).

In this study, the effect of ionic strength in the range of 0-1 M NaCl on CLAR adsorption was evaluated. When the ionic strength of the solution was adjusted to contain 0.01 M NaCl, the adsorption capacity of all MPs decreased significantly (Figure 10). When salinity increases, the adsorption capacity decreases because Na⁺ ions electrostatically bind to the negatively charged PET-MPs and PE-MPs, disrupting the charge balance of the surface and reducing the binding sites of the antibiotic (Atugoda *et al.* 2020). Guo *et al.* (2019) found that the amount of sulfamethoxazole (SMT) adsorption onto MPs decreased with increasing salinity, revealing the importance of electrostatic reaction in the sorption process. Besides, high Na⁺ concentrations increase the density and viscosity of the solution and prevent the movement of analyte

from the solution to the surface of MPs (Zhang *et al.* 2020). However, when the ionic strength of the solution in this study reached up to 1 M NaCl the adsorption capacity of all MPs increased compared to other ionic strength experiments, which can be explained by “salting out” effect. The presence of salt ions reduces the solubility of CLAR, increases its hydrophobic interactions with MPs, and thus induces the “salting out” effect. Ma *et al.* (2019) reported that, when the NaCl content increased from 8.75% to 35%, the adsorption capacity of PVC-S (small PVC particles) for TCS increased by 43.8%, while the adsorption capacity of PVC-L (large PVC particles) for TCS reached to 73.4%. This was primarily explained by the “salting out” effect that occurred during adsorption, which reduced the solubility of TCS in solution and increased the adsorption of TCS onto PVC. At high salinity, PFOS was found to be easily adsorbed on PE and PS, and the sorption of PFOS on MPs in seawater was also explained by this effect (Joo *et al.* 2021).

4. Conclusions

This study has shown that the risk posed by microplastics in aquatic environments is not only due to their chemical content, but also that microplastics have the potential to accumulate antibiotics in water by adsorbing them onto their surfaces. In this study, it was demonstrated that the most common MPs types, PET and PE, have the potential to adsorb the widely used antibiotic CLAR. It has been determined that the adsorption of antibiotics onto microplastics depends on solution pH and ionic strength. The highest CLAR adsorption on PET and PE surfaces occurred when the solution pH was 6-7. The presence of salt ions reduced the solubility of CLAR, increased its hydrophobic interactions with MPs, and thus enhanced the adsorption. The sorption behavior of MPs was also influenced by their type and size. Smaller sizes of MPs and PE type had higher adsorption potential of CLAR. Adsorption of antibiotics on MPs has the potential of vectorial translocation of these chemicals and provides a surface for the formation of antibiotic-resistant genes. In this context, the entry of both plastics and antibiotics into aquatic environments should be prevented.

Acknowledgments

This study was supported by Necmettin Erbakan University, Scientific Research Projects Coordination Office with project number of 23YL19007.

AUTHOR DECLARATION

Funding

This study was supported by Necmettin Erbakan University, Scientific Research Projects Coordination Office with project number of 23YL19007.

Competing interests

We wish to confirm that there are no known conflicts of interest related to the work submitted for publication

Author contributions

Two of the authors contributed to the study conception and design. Material preparation, data collection and analysis were performed by Zainab Ikram Sedeeq SEDEEQ, Fatma BEDUK. The first draft of the manuscript was written by Fatma BEDUK and Zainab Ikram Sedeeq commented on previous versions of the manuscript. We confirm that the manuscript has been read and approved by all named authors and that there are no other persons who satisfied the criteria for authorship but are not listed. We further confirm that the order of authors listed in the manuscript has been approved by all of us. We confirm that we have given due consideration to the protection of intellectual property associated with this work and that there are no impediments to publication, including the timing of publication, with respect to intellectual property. In so doing we confirm that we have followed the regulations of our institutions concerning intellectual property.

We understand that the Corresponding Author is the sole contact for the Editorial process (including Editorial Manager and direct communications with the office). She is responsible for communicating with the other authors about progress, submissions of revisions and final approval of proofs. We confirm that we have provided a current, correct email address which is accessible by the Corresponding Author and which has been configured to accept email from (fabeduk@erbakan.edu.tr)

28.09.2024

Ethical approval

Experimental studies performed in this research study do not involve human or animal participants, neither their organs/tissues etc. No ethical approval is required

Consent to participate

Experimental studies performed in this research study do not involve human or animal participants, neither their organs/tissues etc. No consent to participate is required.

Consent to publish

No individuals participated in this research study. No Consent to Publish is required.

The Data availability statement (DAS)

Data is available on request from the corresponding author.

References

- Ahmad M., Li J.L., Wang P.D., Hozzein W.N. and Li W.J. (2020). Environmental perspectives of microplastic pollution in the aquatic environment: a review, *Marine Life Science and Technology*, **2**, 414–430.
- Arienzo M., Ferrara L. and Trifuoggi M. (2021), The dual role of microplastics in marine environment: Sink and vectors of pollutants, *Journal of Marine Science and Engineering*, **9**(6), 642.
- Atugoda T., Wijesekara H., Werellagama D.R.I.B., Jinadasa K.B.S.N., Bolan N.S. and Vithanage M. (2020). Adsorptive interaction of antibiotic ciprofloxacin on polyethylene

- microplastics: Implications for vector transport in water, *Environmental Technology and Innovation*, **19**, 100971.
- Aydin S., Aydin M.E., Ulvi A. and Kilic H. (2019), Antibiotics in hospital effluents: occurrence, contribution to urban wastewater, removal in a wastewater treatment plant, and environmental risk assessment, *Environmental Science and Pollution Research*, **26**(1), 544–558.
- Baumann M., Weiss K., Maletzki D., Schüssler W., Schudoma D., Kopf W. and Kühnen U. (2015). Aquatic toxicity of the macrolide antibiotic clarithromycin and its metabolites, *Chemosphere*, **120**, 192–198.
- Chen Y., Li J., Wang F., Yang H. and Liu L. (2021), Adsorption of tetracyclines onto polyethylene microplastics: A combined study of experiment and molecular dynamics simulation, *Chemosphere*, **265**, 129133.
- Cole M., Lindeque P., Halsband C. and Galloway T.S. (2011), Microplastics as contaminants in the marine environment: A review. *Marine Pollution Bulletin*, **62**(12), 2588–2597.
- Decision (EU) 2018/840 of 5 June 2018 Establishing a Watch List of Substances for Union-wide Monitoring in the Field of Water Policy Pursuant to Directive 2008/105/EC of the European Parliament and of the Council and Repealing Commission Implementing Decision (EU) 2015/495
- Dovbeshko G.I., Gridina N.Y., Kruglova E.B. and Pashchuk O.P. (2000), FTIR spectroscopy studies of nucleic acid damage, *Talanta*, **53**(1), 233–46.
- Freundlich H.M.F. (1906). Over the adsorption in solution, *Journal of Physical Chemistry*, **57**, 385471.
- Fu L., Li J., Wang G., Luan Y. and Dai W. (2021). Adsorption behavior of organic pollutants on microplastics, *Ecotoxicology and Environmental Safety*, **217**, 112207.
- Guo X., Liu Y. and Wang J. (2019), Sorption of sulfamethazine onto different types of microplastics: A combined experimental and molecular dynamics simulation study, *Marine Pollution Bulletin*, **145**, 547–554.
- Ho Y.S. and McKay G. (1999). Pseudo-second order model for sorption processes, *Process Biochemistry*, **34**(5), 451–465.
- Imwene K.O., Ngumba E. and Kairigo P.K. (2022). Emerging technologies for enhanced removal of residual antibiotics from source-separated urine and wastewaters: A review, *Journal of Environmental Management*, **322**, 116065.
- Joo S.H., Liang Y., Kim M., Byun J. and Choi H. (2021). Microplastics with adsorbed contaminants: *Mechanisms and Treatment*, *Environmental Challenges*, **3**, 100042.
- Klavins M., Klavins L., Stabnikova O., Stabnikov V., Marynin A., Anson-Bertina L., Mezulis M. and Vaseashta A. (2022). Interaction between Microplastics and Pharmaceuticals Depending on the Composition of Aquatic Environment, *Microplastics*, **1**(3), 520–535.
- Langmuir I. (1918). The adsorption of gases on plane surfaces of glass, mica and platinum, *Journal of American Chemical Society*, **40**(9), 1361–1403.
- Li C., Busquets R. and Campos L.C. (2020). Assessment of microplastics in freshwater systems: A review, *Science of the Total Environment*, **707**, 135578.
- Li J., Zhang K. and Zhang H. (2018). Adsorption of antibiotics on microplastics, *Environmental Pollution*, **237**, 460–467.
- Lionetto F. and Esposito Corcione C. (2021). An overview of the sorption studies of contaminants on poly (Ethylene terephthalate) microplastics in the marine environment, *Journal of Marine Science and Engineering*, **9**(4), 445.
- Liu D., Xu Y.Y., Junaid M., Zhu Y.G. and Wang J. (2022). Distribution, transfer, ecological and human health risks of antibiotics in bay ecosystems, *Environmental International*, **158**, 106949.
- Ma J., Zhao J., Zhu Z., Li L. and Yu F. (2019). Effect of microplastic size on the adsorption behavior and mechanism of triclosan on polyvinyl chloride, *Environmental Pollution*, **254**, 113104.
- Moura D.S., Pestana C.J., Moffat C.F., Hui J., Irvine J.T.S., Edwards C. and Lawton L.A. (2022). Adsorption of cyanotoxins on polypropylene and polyethylene terephthalate: Microplastics as vector of eight microcystin analogues, *Environmental Pollution*, **303**, 119135.
- Movasaghi Z., Rehman S. and Rehman I.U. (2008). Fourier transform infrared (FTIR) spectroscopy of biological tissues, *Applied Spectroscopy Reviews*, **43**(2), 134–179.
- Nguyen T.B., Ho T.B.C., Huang C.P., Chen C.W., Hsieh S.L., Tsai W.P. and Dong C.D. (2021), Adsorption characteristics of tetracycline onto particulate polyethylene in dilute aqueous solutions, *Environmental Pollution*, **285**, 117398.
- Pacheco E.B.A.V., Ronchetti L.M. and Masanet E. (2012). An overview of plastic recycling in Rio de Janeiro, *Resources Conservation and Recycling*, **60**, 140–146.
- Shen X.C., Li D.C., Sima X.F., Cheng H.Y. and Jiang H. (2018). The effects of environmental conditions on the enrichment of antibiotics on microplastics in simulated natural water column, *Environmental Research*, **166**, 377–383.
- Zhang H., Wang J., Zhou B., Zhou Y., Dai Z., Zhou Q., Christie P., Luo Y. (2018). Enhanced adsorption of oxytetracycline to weathered microplastic polystyrene: Kinetics, isotherms and influencing factors, *Environmental Pollution*, **243**, 1550–1557.
- Zhang J., Chen H., He H., Cheng X., Ma T., Hu J., Yang S., Li S. and Zhang L. (2020). Adsorption behavior and mechanism of 9-Nitroanthracene on typical microplastics in aqueous solutions, *Chemosphere*, **245**, 125628.
- Zhang M.Q., Zhang J.P. and Hu C.Q. (2022), A Rapid Assessment Model for Liver Toxicity of Macrolides and an Integrative Evaluation for Azithromycin Impurities, *Frontiers in Pharmacology*, **13**, 860702.